Alexandria Engineering Journal (2022) 61, 6769–6783

HOSTED BY

Alexandria University

Alexandria Engineering Journal

www.elsevier.com/locate/aej
www.sciencedirect.com

Experimental investigation on the thermo-hydraulic performance of air–water two-phase flow inside a horizontal circumferentially corrugated tube

Hamdi Ayed [a,b], Akbar Arsalanloo [c], Saleh Khorasani [c,*], Mohammad Mehdizadeh Youshanlouei [d], Samad Jafarmadar [c,*], Majid Abbasalizadeh [c], Fahd Jarad [e,f,*], Ibrahim Mahariq [g]

[a] Department of Civil Engineering, College of Engineering, King Khalid University, Abha 61421, Saudi Arabia
[b] Higher Institute of Transport and Logistics of Sousse, University of Sousse, Sousse 4023, Tunisia
[c] Department of Mechanical Engineering, Faculty of Engineering, Urmia University, Urmia, Iran
[d] Faculty of Mechanical Engineering, Urmia University of Technology, Urmia, Iran
[e] Department of Mathematics, Cankaya University, Etimesgut, Ankara, Turkey
[f] Department of Medical Research, China Medical University Hospital, China Medical University, Taichung, Taiwan
[g] College of Engineering and Technology, American University of the Middle East, Kuwait

Received 19 June 2021; revised 2 December 2021; accepted 7 December 2021
Available online 18 December 2021

KEYWORDS

Corrugated tube;
Non-boiling air–water two-phase flow;
Heat transfer coefficient;
Flow visualization;
Pressure drop

Abstract In this study, flow visualization, pressure drop and thermal characteristics of the corrugated tube with non-boiling air–water two-phase flow were experimentally studied. Glass tubes were used to visualize the flow patterns of two-phase flow. Furthermore, the thermal behavior of two phase flow was studied in the copper made tubes which was under constant heat flux. The total of 740 W thermal energy was applied on tubes. Superficial velocity of liquid was within the range of 0.42 m/s to 1.69 m/s. Also, the superficial velocity of air was within the range of 0.21 m/s to 1.06 m/s. The results revealed that the corrugations significantly affect the flow patterns which results in earlier transition. The flow patterns of bubbly, churn, wavy slug, wavy plug, wavy stratified and mist flow were observed inside corrugated tube. Also, it was found that the maximum Nusselt number increment in corrugated tube was 3%. Besides, formation of the mist flow in corrugated tube reduced the Nusselt number. Also, the pressure drop was significantly affected by the air–water two-phase flow presenting around 165 % in the pressure drop compared to the single phase flow.

* Corresponding authors at: Department of Mathematics, Cankaya University, Etimesgut, Ankara, Turkey (F. Jarad).
E-mail addresses: hayed@kku.edu.sa (H. Ayed), akbar.arsalanloo@gmail.com (A. Arsalanloo), Khorasani.saleh@yahoo.com (S. Khorasani), S.jafarmadar@urmia.ac.ir (S. Jafarmadar), m.abbasalizadeh@urmia.ac.ir (M. Abbasalizadeh), fahd@cankaya.edu.tr (F. Jarad), ibrahim.maharik@aum.edu.kw (I. Mahariq).

Peer review under responsibility of Faculty of Engineering, Alexandria University.

https://doi.org/10.1016/j.aej.2021.12.024
1110-0168

Nomenclature

Q	Total gained thermal energy by working fluid (J)
L	Length of tube (m)
D_i	Inner diameter of tube (m)
D_o	Outer diameter of tube (m)
P	Corrugation pitch in corrugated tube (m)
d	Depth of corrugation (m)
Q_g	Gas (air) flow rate (lit/min)
Q_l	Liquid (water) flow rate (lit/min)
$T_{w.i}$	Mean wall temperature (°C)
$\dot{m}$	Mass flow rate (Kg/s)
Nu	Dimensionless convective heat transfer coefficient (Nusselt number)
c	Specific heat (J/Kg. K)
K	Conductive heat transfer coefficient (tube)
T_{in}	Inlet temperature (°C)
T_{out}	Outlet temperature (°C)
$A_{l.1}$	Cross section of tube occupied by liquid phase when the flow was single phase(m^2)
$A_{l.2}$	Cross section of tube occupied by liquid phase when the flow was Two phase(m^2)
f	Friction factor
Re	Reynolds number
$h_{overall}$	Convective heat transfer coefficient
V_{sl}	Superficial velocity of the liquid phase (m/s)
V_{sg}	Superficial velocity of the gas phase (m/s)
$V_{l.1}$	Actual velocity of the liquid phase when the flow was single phase(m/s)
$V_{l.2}$	Actual velocity of the liquid phase when the flow was two phase(m/s)
A	Heat transfer surface of tube (m^2)
$A_{l.1}$	Actual velocity of the liquid phase when the flow was single phase(m^2)
$A_{l.2}$	Actual cross section of the liquid phase when the flow was two phase(m^2)
T_{wi}	Inner wall temperature (calculated) (°C)
T_{wo}	Outer wall temperature (measured) (°C)
ΔP	Pressure drop (Pa)
X	Independent variable
W	Uncertainty
T_b	Bulk temperature of fluid flow
R	Dependent variable
k_f	Conductive heat transfer coefficient of liquid in viscous layer
Ac	Heat transfer area for corrugated tube
As	Heat transfer area for smooth tube

Abbreviations

sp	single phase
c	Corrugated tube
g	Gas phase
l	Liquid phase
s	Smooth tube
tp	two phase

1. Introduction

Most recently, corrugated tubes have been introduced as an effective heat transfer enhancement method. The improved thermal performance and anti-fouling nature of corrugated tubes make them an attractive choice for experts and engineers to be used instead of smooth tubes in many industrial applications as like to gas/oil refinery systems, chemical engineering processes, food and production applications, etc., [1-3]. Most of these industrial applications include a form of multi-phase flow at which the gas/liquid two-phase flow is the most dominant form of them. Besides, recent studies have proposed the gas/liquid two-phase flow as an active heat transfer enhancement technique [4,5]. Due to the different nature of gas/liquid two-phase flow compared to single-phase flows, improved thermal performance of two-phase flows and the existence of these flows in nature and many industrial applications, numerous experts have tried to investigate the properties of such flows inside the smooth tubes. Since the characteristics of gas/liquid two–phase flow differs with changes at the ratio of two phases, form, shape and the orientation of the passing tube, investigations on defining the effect of mentioned parameters are significantly valuable. In the following a summarized literature of recent investigations on the gas/liquid two-phase flows and the application of corrugated tubes is presented.

For the horizontal orientation of tube, numerous investigations have been performed to study the gas/liquid two-phase flow in the smooth tubes. Kim and Ghajar [6] performed experimental investigations to study the flow patterns and thermo-frictional properties of gas/liquid two-phase flow in the horizontal smooth tube. They reported that the addition of the gaseous phase into the liquid stream enhances the interaction of the phases which results in turbulence level and mixing action enhancement which augments the heat transfer coefficient. However, further addition of air creates a maximum in the heat transfer coefficient for a fixed amount of liquid superficial Reynolds. In another study, Kim and Ghajar [7] developed an experimental equation to predict the heat transfer coefficient of the two-phase flow inside the horizontal tube. Their study aimed to present a correlation that could predict the heat transfer coefficient in all range of flow patterns in the horizontal tube. They proposed new correction factors, in order to rectify the previously proposed correlations. López et al [8] performed an experimental and numerical study to investigate the characteristics of the gas–liquid two phase flow inside the horizontal pipes. For the experimental study, they used a high-speed filming (HSF) method and simulation was performed by means of the Volume Of Fluid (VOF) method. They reported good agreement between the experimental and numerical results especially for the slug and annular flow patterns. The structure of intermittent flow inside a horizontal smooth tube was studied by Thaker and Banerjee [9]. They proposed new correlations for predicting the flow characteristics of intermittent flow. Flow characteristics of gas/liquid two-phase flow inside an annulus were studied by Ibarra et al. [10,11]. They considered two cases for the annulus. In the first case, the inner tube was placed in concentric condition and at the second case the inner tube was placed at eccentric condi-

tion (the inner tube was placed on the bottom wall of the outer tube). Their results revealed that the slug flow was the most dominant form of the two-phase flow happening at the mentioned orientation of annulus. Investigations have presented that the orientation and form of the tubes have a significant effect on the characteristics of the two-phase flow. The characteristics of two-phase flow in the downward inclined tube were investigated by Bhagwat and Ghajar [12] who considered the inclination angle ranging from -5° to -90°. Their findings presented that the inclination has a significant effect on the transition between stratified and slug/intermittent flow patterns. Also, they reported that the negative inclination has more effect on the buoyancy-driven interfaces of the two-phase flow. In another study, Bhagwat and Ghajar [13] performed an experimental study to investigate the effect of positive inclination on the properties of gas–liquid two-phase flow. They considered the inclination angle range of $+5^{\circ}$ to $+90^{\circ}$. Their results revealed that the increment in the inclination has a remarkable effect on void fraction, heat transfer coefficient and total pressure drop at low liquid and gas flow rates. Liu and Hibiki [14] investigated the upward two-phase flow at tubes with vertical orientations. They focused on transition criteria of different flow patterns and classified the flow regime into 6 distinct flow regimes which are bubbly, finely dispersed bubbly, cap bubbly, cap turbulent, churn, and annular flows. In another study, Wu et al. [15] investigated the two-phase flow within a vertical annulus. They considered two different test sections with different diameters. Their results presented that the annular flow does not develop within the vertical annuli. Interfacial friction of annular flow in the upward two-phase flow was studied by Aliyu et al. [16]. They proposed an empirical correlation for predicting the interfacial friction. In order to better fit the wide range of experimental results, they used dimensionless numbers for considering the effect of the tube diameter. Investigations on two phase flow inside the vertical annulus have shown that the flow regimes for large diameter and narrow diameters annuluses are the same. However, the transition criteria for each type of annuluses were different. It was found that the transition from slug to churn flow has happened in low superficial gas velocities compared to that in large diameter annuluses [17,18]. Gourma and Verdin [19] simulated the slug flow in the horizontal helical tube. Their findings presented that installing helical pipes at the upstream of large scale devices could potentially decrease the number of slugs. In another study, Zhu et al. [20] performed an experimental investigation and studied the characteristics of intermittent flow inside helical tubes with three different coil diameters. Their findings revealed that the slug length decreases as the coil diameter decreases due to the enhancement of Dean vortices. Moradi et al. [21] investigated the thermal properties of upward gas liquid two-phase in a helical tube. They reported that slug flow within the helical tube could increase the heat transfer coefficient up to 35%. Saisorn et al [22] worked on heat transfer characteristics of two-phase flow in a horizontal micro-channel and reported that up to 80% heat transfer enhancement can be achieved. They also reported greater heat transfer characteristics in slug flow in comparison with gas core flow.

Due to the enhanced thermal performance and anti-fouling nature of the corrugated tubes, experts and engineers are willing to use such tubes in many industrial applications. Consequently, numerous investigations have been performed to study the design parameters and characteristics of flow inside the corrugated tubes. Cancan et al. [22] worked on heat transfer enhancement and pressure drop of a coiled corrugated tube with corrugations of spherical shape using numerical simulations. Dizaji et al. [23] investigated the effect of both concave and convex corrugations on the performance of a double pipe heat exchanger and reported up to 117% enhancement heat transfer rate due to corrugations. Qi et al. [24] conducted an experimental investigation and studied the effect of using TiO_2-water nano fluid on the thermal performance of a corrugated tube. They reported that using TiO_2 could increase the heat transfer rate by up to 53.95%. Andrade et al. [25] studied the effect of helical corrugation on the thermal enhancement and reported that the corrugation is more effective at the transitional flow regime. Their results presented up to 4.7 times increment at the Nusselt number amounts compared to that of a smooth tube. Ajeel et al. [26] utilized trapezoidal corrugations in a numerical simulation to find efficient geometrical parameters to promote thermal performance. Xin et al. [27] numerically investigated the thermo-frictional properties of oscillatory flow in the spirally corrugated tube. Their results revealed that using two start spiral corrugations could increase the heat transfer rate up 36%.

As mentioned before and based on the literature, it could be deduced that the form, shape, size, and orientation of tubes could potentially affect the characteristics of two-phase flow. Besides, the increasing usage of corrugated tubes in the industry and the presence of gas/liquid two-phase flow in industrial applications necessitates investigations on the behavior of gas/liquid two-phase flow in the corrugated tubes. Hence, it could be concluded that the heat transfer in two-phase non-boiling flow has been addressed from many different aspects in the literature and many other works have been dedicated to characterize the heat transfer enhancement in corrugated tubes, while to the authors' best knowledge no previous study has ever addressed the simultaneous application of non-boiling two-phase flow in a circumferentially corrugated tube. Consequently, the necessity of the present investigation is based on the lack of investigations on the thermal performance of the gas–liquid two phase flow inside corrugated tubes. Since the enhanced tubes (especially corrugated tubes) are attracting attention to be used in applications that include gas/liquid two phase flow and there is lack of evaluations in this regard the investigations on the present issue are very important. In this work, we have presented the visualization of various flow patterns formed in two-phase flow with various air and water superficial velocity in a corrugated tube. The pressure drop and heat transfer characteristics have been presented and the mechanisms contributing to heat transfer characteristics in different flow patterns have also been discussed.

2. Experimental setup and data reduction

2.1. Experimental setup

A schematic of the test setup is presented in Fig. 1. The test apparatus is comprised of 13 distinct elements which are as follows: 1. Water Reservoir, 2. Water Pump, 3. Water Rotameter, 4. Air Compressor, 5. Air Rotameter, 6. Control Valves, 7. Test Tube, 8. Manometer, 9. Heater, 10. K-Type thermocou-

ples, 11. Data Logger, 12. Voltage Regulators, 13. Multimeter. These series of tests were taken in an open-loop flow system in which a reservoir is used to store the fed water. The water was pumped from the reservoir into a T-junction where the compressed air entered its other branch perpendicular to the water stream to get mixed within the T-junction. It is worth mentioning that a U shaped oil trap was utilized to avoid any probable oil contamination of the air compressor. The water and air were mixed in the T-junction and then passed into tube. It is noteworthy that between the T-junction and entrance of the tube, there was a 70 cm distance which allowed the flow to completely get mixed. Also, this distance ensured that the two phase flow at the entrance of the tube was completely developed [28]. It is also worth noting that the camera was placed at 60 cm from the inlet of the tube. A schematic of the T-junction and air injection mechanism is explained in the work of Khorasani et al. [25] and is omitted here for the sake of brevity. Both air and water flow rates were measured by the water and air rotameters. The water–air mixture enters the test tube which was heated by a wire heating element. The heaters were wrapped on the outside of the copper tube. The thermal energy produced by the elements was kept constant in all tests by using a dimmer to set the voltage of heaters and at the same time monitoring the current on a multimeter to make sure that there is no variation in the current. Surfaces of both corrugated and smooth test tubes were covered with a layer of aluminum foil to have an efficient dispersion of thermal energy on the surface. It should be noted that for fabricating the corrugated tube a smooth tube was pressurized in some point (defined based on the pitch of the corrugation). This method does not change the surface of the heat transfer and just pushes the material into the inner part of the tube. Consequently, the heat transfer surface for both the smooth and corrugated tube was equal. Fig. 2 B present the mentioned methodology used for fabricating the corrugated tube. For the insulation, three layers of glass wool were used to insulate the tube in order to avoid heat losses. Copper is chosen as the material for both corrugated and smooth test sections and flow visualization was performed using corrugated and smooth glass tubes of the same geometrical characteristics. Both corrugated and smooth copper and glass tubes have the same length, inner and outer diameters. To calculate the overall convective heat transfer coefficient, 7 K-type thermocouples are used to measure the surface temperatures and two sensors of the same type are used to measure the temperatures of the inlet and outlet flow. The Fig. 2 C presented the schematic of the location of thermocouples that were used to measure the outer wall temperatures. As is shown, the thermocouples had the distance of 28 cm with each other. Besides, each consecutive thermocouple had the radial distance of 180 °C. To ensure that the thermocouples were just sensing the surface temperature, the thermos couples was covered by glass-wool insulation. It should be noted that the utilized method was used by numerous researchers that have conducted similar researchers [29-31] which presents that the mentioned methodology is highly credible from the viewpoint of researchers. Also, it should be noted that since the deviation of surface temperature between the beginning of the tube and the end of tube was less than 12 °C (It should be noted that the total thermal energy applied to surface of tube was only about 740 W), 7 thermocouples were completely enough to measure the surface temperature. Indeed, each two thermocouples was associated with a roughly temperature deviation of 1.5 °C which presents the credibility of using 7 thermocouples.

The corresponding data of temperature and pressure drop were collected using a 12 channel Lutron (BTM4208SD) data logger and Lutron manometer (PM-9100), respectively. In each test, the temperatures were recorded after the thermal stability was achieved. It is to be noted that for the data logger has the calibration card. Also, for finding the Cold reference temperature an ice-water bath was used before performing the tests. Also, it should be noted that the place where the tests

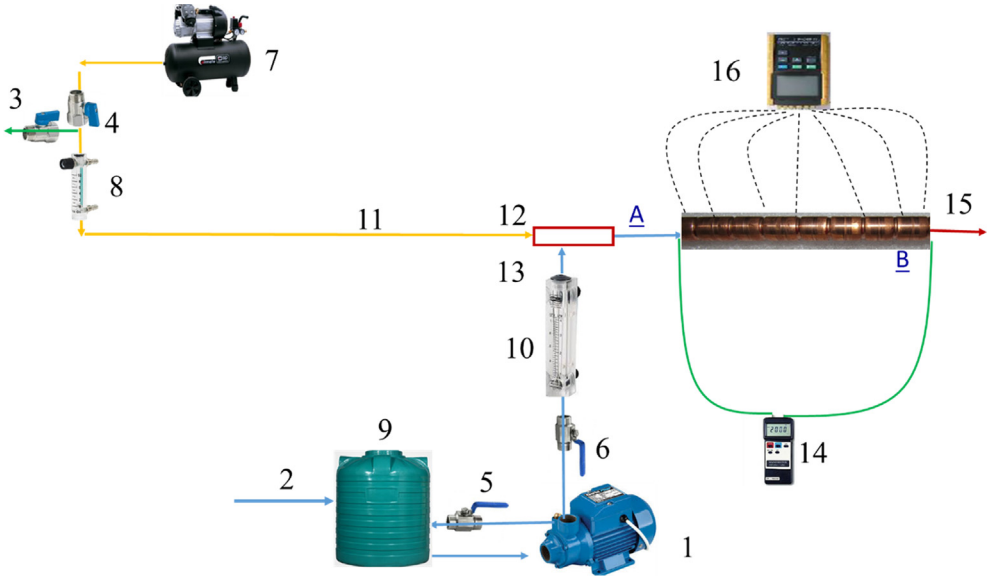

Fig. 1 Schematic view of the set up configuration: 1- Water pump; 2-Tap water; 3-Air Bypass flow; 4-Control valves; 5-Water Bypass flow; 6-Control valves; 7-Air compressor; 8-Air Rotameter; 9-Resevoir; 10- Water rotameter; 11-Air flow; 12-Mixing well; 13-Water flow; 14-Manometer; 15 -Out flow.16- Data logger.

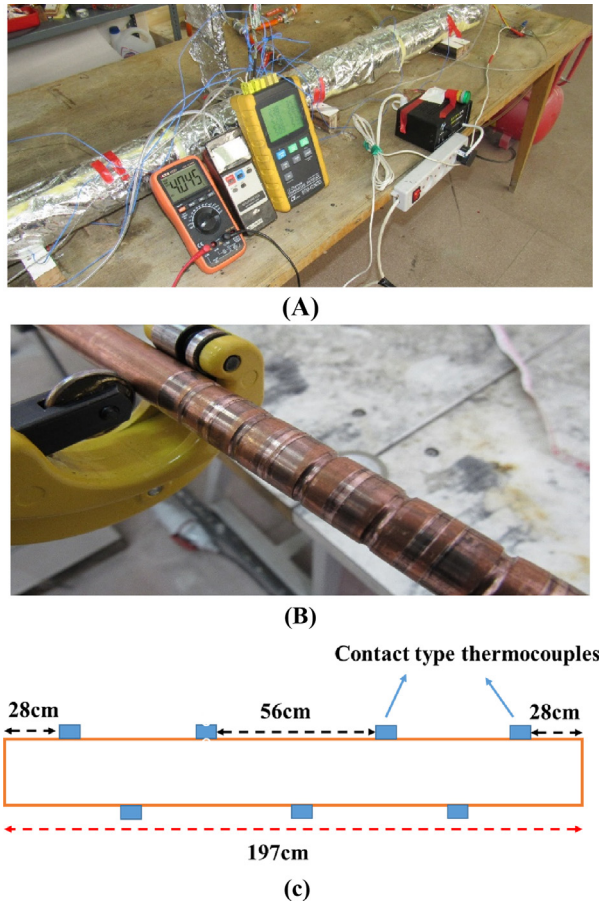

Fig. 2 (A) General view of setup; (B) fabrication of corrugations.

were carried out was an academic lab where the impurities of the water were controlled using filters that were fabricated on the water line. So, the effect of impurities of the water was considered to be negligible.

The tests were performed for water flow rates of 2, 4, 6, and 8 lit/min which are associated with the superficial velocity of 0.42, 0.84, 1.27, and 1.69 m/s (providing Reynolds number within the range of 2691 and 16900, which was within turbulent regime). For each water flow rate, three air flow rates of 1, 3, and 5 lit/min were used which are associated with the superficial velocity of 0.21, 0.63, and 1.06 m/s. The water and air entered the system at around 15 °C and 24 °C , respectively. Also, 740 W energy was applied on the surface of copper made tubes which provided a density of 980 W/m^2 thermal energy. The initial data was recorded after the tests received the thermally stable condition. It should be noted that each test took a rough time of 40 min to receive the thermal stable condition. It is to be mentioned that as the density of air is very small, the mass flow rate of air is much less than that of the water flow and as the specific heat capacity of air is less than water, the heat transfer between air and water can be assumed negligible. The setup configuration is depicted in Figs. 1 and 2 and the geometric characteristics of the tubes are presented in Table 1. Fig. 3 shows a general view of both smooth and corrugated, copper, and glacial tubes used in this study.

2.2. Data reduction

The heat transfer coefficient in this study was calculated based on the constant heat flux boundary condition. For this, the wall temperatures and bulk temperature of the flow at the inlet and outlet of the test section were measured. The outer wall temperature of the tube was measured at 7 points. Then the inner wall temperature was predicted based on the wall resistance of the tube and the average of these 7 points was used in calculations. The following process was followed up to calculate the heat transfer coefficient.

The increase in internal energy of the fluid is calculated through the following equation:

$$Q = \dot{m}.C.(T_{in} - T_{out}) \tag{1}$$

In the above equation, $\dot{m}$ is the mass flow rate and C is the specific heat capacity of water. T_{in} and T_{out} are the temperature of the inlet and outlet flow respectively. The convective heat transferred to fluid is expressed by Newton's law of cooling which is as follows:

$$Q = h_{overall} * A * (\bar{T}_{wi} - \bar{T}_b) \tag{2}$$

Which h is the overall convective heat transfer coefficient with A being the surface of the tube through which the heat has been transferred to the fluid. For the considered value of the heat transfer area, it should be noted that the considered are was almost equal to the smooth tube. since the corrugated tube was made by pressurizing the smooth tube and the change in active surface area was negligible. Nevertheless, the authors have tried to considered any change the Eq. (3) was used for calculating the heat transfer area for corrugated tube.

$$A_C = A_{smooth} + (4\pi d(D - 2d) - 2\pi dD) * \frac{l}{P} \tag{3}$$

Which d is the corrugation depth, D is the diameter of the tube, l is the tube length and P is the corrugation pitch. By equating the Eqs. (2) and (1), the overall heat transfer coefficient is calculated as:

$$h_{overal} = (\dot{m}C(T_{out} - T_{in}))/(A_{S/C}(\bar{T}_{wi} - T_b)) \tag{4}$$

In this equation As is referred to heat transfer area of smooth tube and Ac is referred to heat transfer area of corrugated tube. T_b is called the bulk temperature and is calculated as follows:

$$T_b = (T_{out} + T_{in})/2 \tag{5}$$

Where, T_{out}andT_{in} are the outlet and inlet temperature of tube.

In the above equations, $\bar{T}_{wi}$ is the average of the temperatures of the tube inner surface which is calculated based on the tube outer temperature and conductive resistance of the copper-made tube.

Table 1 Geometrical characteristics of tubes.

Length of tube	L (mm)	1970
Inner diameter	D_i (mm)	10
Outer diameter	D_o (mm)	12.7
Corrugation pitch	P (mm)	15
Depth of corrugation	d (mm)	1

Fig. 3 Glass and copper made tubes (corrugated and smooth).

$$T_{wi} = T_{wo} - \frac{Q \ln\left(\frac{D_o}{D_i}\right)}{2\pi KL} \tag{6}$$

$$\bar{T}_{\text{wi.mean}} = \left(\sum_{i=1}^{7} (T_{wi})_i\right)/7 \tag{7}$$

Consequently, the average Nusselt number could be calculated as follow:

$$Nu = \frac{h_{\text{overal}} D_{h.s/c}}{k_f} \tag{8}$$

In the above equation, $D_{h.s/c}$ and the k_f are the hydraulic diameter (associate with smooth tube and corrugated tube) and conductive heat transfer coefficient. It should be noted that for the for the hydraulic diameter, the of the corrugated tube, the average of maximum diameter and minimum diameter was used as the hydraulic diameter. Also it should be noted that the considered method for calculating the heat transfer coefficient was previously used by other researchers as like to references [28,32,33].

Furthermore, the results are presented in terms of the superficial gas and liquid velocity which are calculated as following equation:

$$v_{sg/sl} = \frac{Q_{l/g}}{A} \tag{9}$$

While the thermocouples have been placed in such a way that they cover all sides of the pipe surface along its length. It should be noted that due to the low thermal capacity of air in comparison with water, the heat transferred by air has been considered negligible, thus the calculations for the injected air is omitted.

Regardless of the precision of measurement instruments and the operator, there is a level of deviation between the measured values and true values which is regarded as an error. To have a rational insight into the deviation within which the true amount of the value lies, the concept of uncertainty is used. In this study, the method proposed by Moffat [34] is employed to evaluate the uncertainty of measurements. This method was widely used by numerous experts as references [21]. The uncertainties are presented in Table 2. It is worth mentioning that the amounts of the uncertainty values for both dependent and independent parameters were in agreement with the aforementioned references [28,32].

2.3. Setup Validation

Before gathering the experimental data, validation tests were performed to ensure the proper functionality of the test apparatus and the reliability of experimental results. The validation is performed for both the friction factor and dimensionless heat transfer coefficient (Nusselt number) based on the empirical correlations and reliable data presented in the literature.

The Blasius and Petukhov correlations [35] have been employed to validate the friction factor data derived from experimental tests. Fig. 4a a shows a comparison between the friction factor calculated by the mentioned correlations and the results of experimental tests. The Blasius friction correlation for Re less than $2*10^4$ is written as follows:

$$f = \frac{0.316}{Re^{\frac{1}{4}}} \tag{10}$$

And the Petukhov friction factor correlation for Reynolds ranging from 3000 to $5*10^6$ is expressed as:

$$f = (0.790 * \ln(Re) - 1.64)^{-2} \tag{11}$$

As seen in Fig. 4.a, the discrepancy observed is about 1% for all points except at V_{sl} = 84 m/s which shows a discrepancy of about 10%. These results show a good agreement between the results of our experimental tests and the results of Blasius and Petukhov correlations.

In Fig. 4b the Nu values of corrugated tube derived from the experimental tests have been compared with the results of Sun and Zeng [1] Rostami et al. [32] which a maximum deviation of 9% is observed. It should also be noted that the experimental apparatus was checked out for heat balance to assure its efficient performance. According to calculations for single phase flow, it was observed that the energy absorbed by the fluid flow was ranging from 694 W to 711 W. This amount of energy was produced by a heater working under operating conditions with voltage of 185 V and current of 4A. The energy waste of the system was estimated to be ranging from of 3.9% to 6.2%. The presented results for the friction factor,

Table 2 Uncertainty of values

Independent variables	
Parameter	Uncertainty
Inlet water temperature (°C)	± 0.5
Inlet air temperature (°C)	± 0.5
Wall temperature (°C)	± 0.5
Water flow rate (lit/min)	± 0.25
Air flow rate (lit/min)	± 0.25
Uncertainty in read values of table (ρ, k, cs,…)	±0.1–0.15%
Dependent variables	
Nusselt number	± 9.75 %
Heat transfer coefficient(W/m^2K)	6.85%
Pressure drop	± 2 %
Produced thermal energy	± 3%

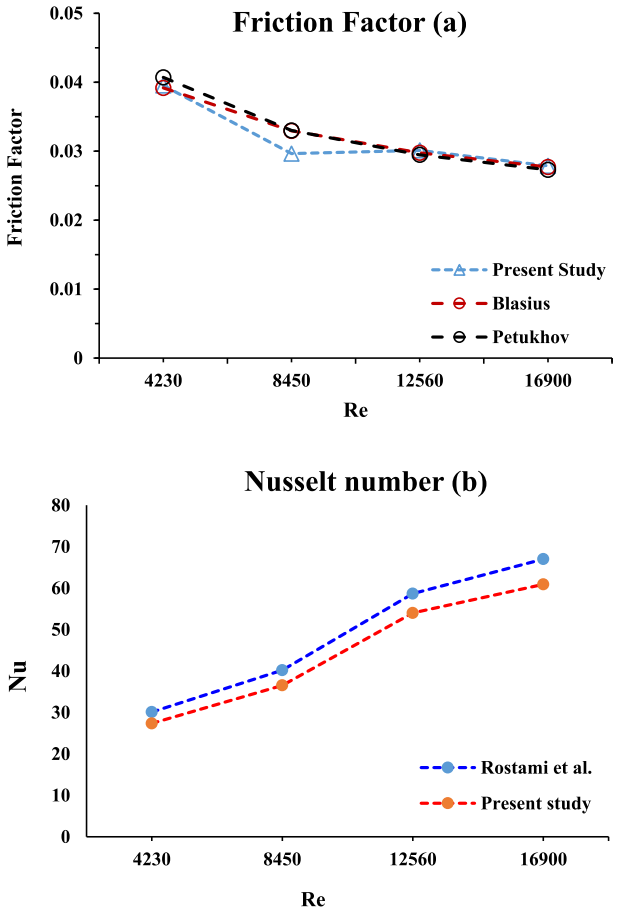

Fig. 4 Validation of results for single phase flow; (a) friction factor, (b) Nusselt number.

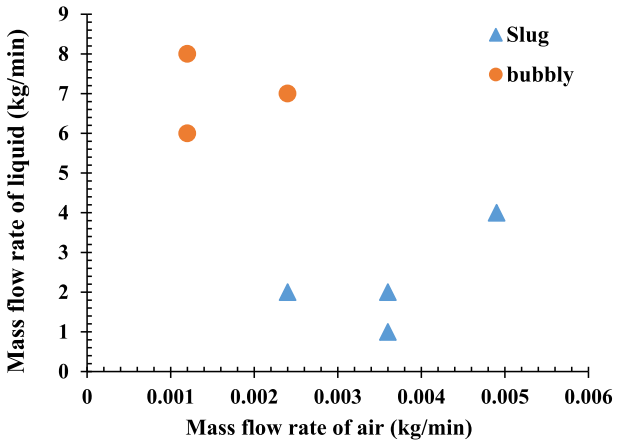

Fig. 5 Various cases consideredd for validation of experimental setup.

Nusselt number and heat balance demonstrate the reliability of the results and the accuracy of the experimental equipment.

Also, to examine the validity of flow pattern results, the patterns of air–water two-phase flow inside a straight tube were compared with the results of Kalapatapu et al.[36]. Fig. 5 exhibits the observed flow patterns for various liquid and gas flow rates. These patterns agree well with those reported by Klapatapu et al.[36].

Fig. 6 shows typical flow patterns depicted in Fig. 3 observed for water flow rate of 1 Lit/min and gas flow rate of 5 Lit/min (Fig. 6a), water flow rate of 5 Lit/min and gas flow rate of 2 Lit/min (Fig. 6b), and water flow rate of 8 Lit/min and gas flow rate of 1 Lit/min (Fig. 6c). It should be noted that comparing the results of the present investigation with previously published papers (as like to Abdulkadir et al.[37] and Darzi and park [38]), it could be concluded that same behavior could be seen for the results of the present investigation too. For example the results of the Abdulkadir et al.[37] presented that the slug flow consists of large air bubble that have wavy interface with the water phase and some tiny bubble follow them at the tail part of slug. Also, the presence of small bubbles that had the size of less than diameter of the tube was observed as the bubbly flow through the results of present study and those mentioned before Abdulkadir et al.[37] Darzi and park [38] and Kalapatapu et al.[36]. As the outcome, the above comparison presented that the flow pattern results of the present investigation is reliable and is in agreement with the previously published articles.

3. Results and discussion

3.1. Flow visualization

Non-Boiling two-phase flow is known to be a useful phenomenon in various industrial applications such as oil and petroleum production industries [6,7]. Also, it has been proposed as a way of heat transfer enhancement technique in heat exchangers [5,39] which makes it important to recognize its characteristics. One way to understand the behavior of two-phase flow is to study the flow patterns and visualize the morphological properties of the phases and their interactions. Many previous studies have focused on visualization of multiphase flows in pipes of different diameters and orientations. However, in this study, the effect of corrugations on the flow patterns of the two-phase air–water mixture in a horizontal corrugated tube was considered which has not been reported in the literature before. The glass tube used for visualization had the same geometrical characteristics as the one used for thermal experiments such as corrugation pitch and depth, inner diameter and etc. The photos have been taken by a Canon SX530 camera with a shutter speed of 1/2000 (s) which was sufficient to freeze the scene and visualize the patterns formed in the two-phase flow.

In this study, various flow patterns including plug flow, slug flow, stratified flow, stratified wavy flow, bubble flow, churn flow and mist flow were observed. At lower air velocity rates, augmentation of velocity of liquid results in formation of smaller bubbles and by further increment of liquid velocity, the flow pattern gradually changes to bubbly flow in smooth tube. This phenomenon is depicted in Fig. 7.a to d which is associated with the liquid velocity ranging from 0.42 m/s to 1.69 m/s at constant air velocity of 0.21 m/s. In Fig. 7a to c, the plug flow pattern was observed in smooth tube while size of air bubbles reduces gradually with the increment of liquid velocity and tends to change to bubbly flow. Plug flow was characterized by sequential formation of long air bubbles [40] that has very smooth interface with the liquid phase and there is no tiny

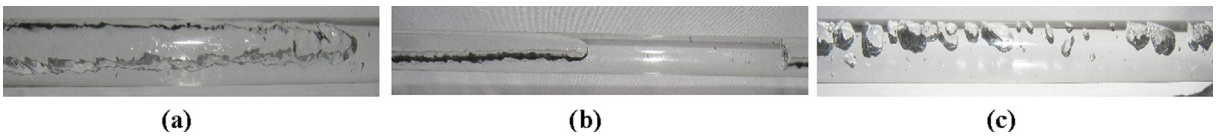

Fig. 6 Typical slug and bubbly flow patterns considered for validation of the experimental setup.

bubbles at the tail part of the plug (for the smooth tube). It should be noted that the formation of the slug and plug flow in this study was very similar to what was reported by Abdulkadir et al.[37].Also, the same type of flow pattern was observed as the prevalent two-phase flow pattern at lower air superficial velocity in corrugated tube (Fig. 7e). The plug flow in corrugated tube had a bit way interface with liquid phase which was because of more shear stress of the liquid phase within corrugated tube. However, the wavy interface of the plug flow in corrugated tube was different with that of slog flow meaning that the plug flow in corrugated tube had less frequent waves. In Fig. 7e wavy plug flow pattern was observed which by the increment of the liquid velocity had tended to alter with churn flow (presented in Fig. 7f). Churn flow was characterized as large gas bubbles being deflected in a chaotic manner which is surrounded by smaller bubbles [14,41]. Further increment of liquid velocity resulted in formation of bubbly flow regime. Comparing the flow patterns in smooth and corrugated tubes in Fig. 7, it was revealed that by raising the liquid velocity at constant air velocity the transition of flow pattern from plug to bubbly flow occurs at faster than the smooth tube. This phenomenon is due to the presence of corrugations. Indeed, as the air bubbles incessantly impact the tube walls and get disrupted to smaller bubbles.

Through the higher air velocity rates, the air bubbles become longer and tend to create a type of flow pattern named as stratified flow (shown in Fig. 8a). In stratified flow, a distinct boundary can be recognized along the horizontal direction while the fluid with higher density is placed at the bottom due to the gravitational effects Kalapatapu et al.[36]. In the same operational conditions through the corrugated tube, the stratified flow turns to stratified wavy flow which is because of the presence of corrugations. By increasing the liquid velocity at Vsg = 1.06, the stratified flow in smooth tube turns to plug flow and later to slug flow as could be seen in Fig. 8b, c and d while in corrugated tube the plug flow in Fig. 8e alters with churn flow in Fig. 8.f and then changes bubbly flow (Fig. 8g) and finally the mist flow was formed at Vsl = 1.69 m/s (Fig. 8h). Mist flow occurs at high velocity of gas and liquid. In this two-phase flow regime, the high shear stress between the gas and liquid interface breaks the liquid continuity and the liquid film turns to separated droplets Gao et al. [42].

It's worth noting that the air bubbles through the smooth tube lean toward the top wall of the tube while in a corrugated tube the bubbles disperse more evenly and occupy all the cross-section of the tube. As known, the inertia and buoyancy forces are the main forces affecting the overall stream of two-phase flow in horizontal tubes [6,7]. In the smooth tubes and especially at low liquid velocity due to laminar form or less turbulent form of the flow, the inertial forces act at the longitudinal direction. Besides, due to the low shear stress of the flow, the air bubbles have bigger size and as a result the buoyancy force has more impact on them. All these together, makes the air bubbles/slugs to move at the top of the tube. However, at the corrugated tubes, the increased shear stress and coincidence with the corrugated parts break the air bubbles into smaller ones. Besides, due to the variation of flow cross-section in corrugated tubes, the direction of the fluid parcels velocity vector as well as inertial force affecting air slugs varies continuously. Less buoyancy force and variable inertial force leads to a more even distribution of air slugs through the cross-section of the corrugated tube. The corrugations, not only break the bubbles and form bubbly flow, but also cause

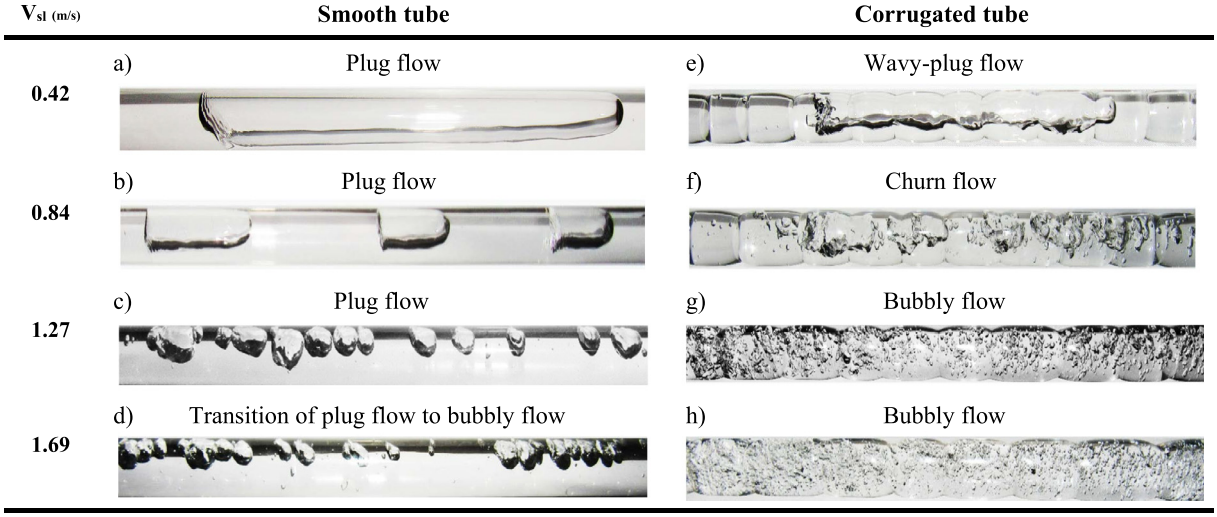

Fig. 7 Presentation of flow patterns for V_{sg} = 0.21 m/s versus different liquid superficial velocity in both smooth and corrugated tubes.

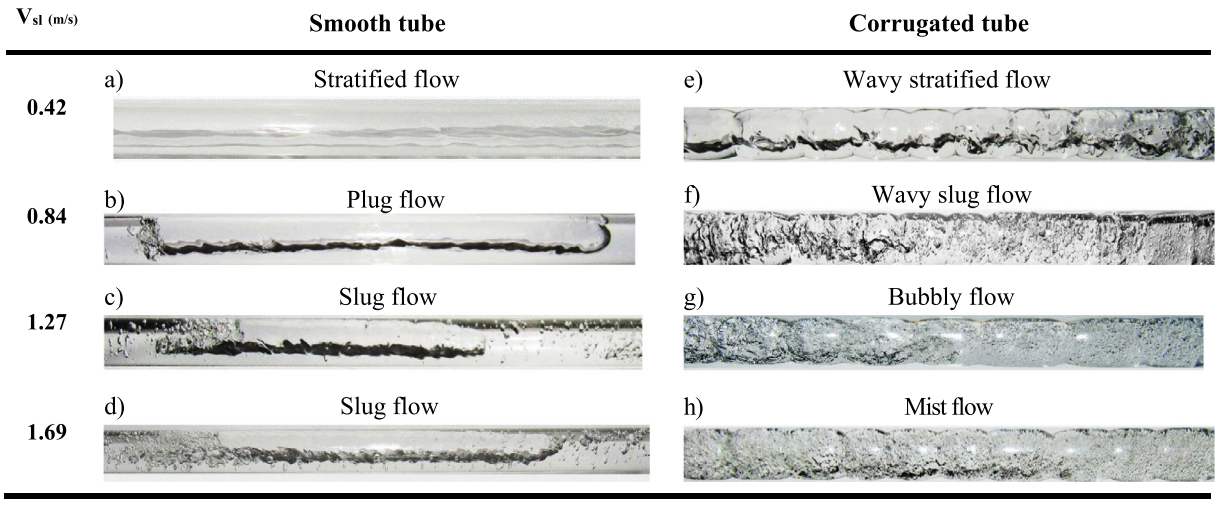

Fig. 8 Presentation of flow patterns for Vsg = 1.06 m/s versus different liquid superficial velocity in both smooth and corrugated tubes.

an intense disorder in the formation and transport of bubbles resulting in the formation of mist flow which can be observed in Fig. 8h. It should be noted that in transition regions it is difficult to distinguish a precise regime of the two-phase flow and in some regions the observations may match more than one flow pattern definition. Hence the map of the flow patterns observed in this study has been presented in Fig. 9 to make it easier to identify effect of superficial velocity of liquid and gas on the flow patterns formed.

3.2. Pressure drop analysis

The results for pressure drop along with both the smooth and corrugated tubes are presented in Fig. 10. A digital manometer was connected to the inlet and outlet of the tube and pressure drop data was obtained. As we have a secondary phase flowing inside the tube, it is natural to have fluctuations in the amount of pressure loss detected by the manometer, hence it is to be noted that the data provided by Fig. 10 is based on the mean values of the pressure loss, while the mean values presented in these figures are the average of maximum and minimum of the pressure loss measured by the digital manometer. Deviation of the data from mean values along with the maximum and minimum of the measured pressure drop is presented in Table 3. Also it should be noted that the maximum uncertainty of the pressure drop was about 2% which was based on the accuracy of the manometer, since the data was recorded by the digital manometer the uncertainty based on the operator skill was neglected. Fig. 10 shows the pressure drop values along both the smooth and corrugated tubes for different superficial velocities of water and air streams. As it is shown, increment of superficial velocity of both water and air flows results in significant increment in the pressure drop. Fig. 11 also indicates the ratio of multiphase flow pressure drop to that of single-phase flow for both smooth and corrugated tubes which provides a better insight that how the second phase affects the pressure drop. Fig. 11.a depicts the ratio of multiphase pressure drop to single-phase pressure drop for a smooth tube based on the air velocity for different water velocities. It is concluded that by the increment of air velocity, the pressure drop ratio has an ascending trend for all water superficial velocities. Also, it

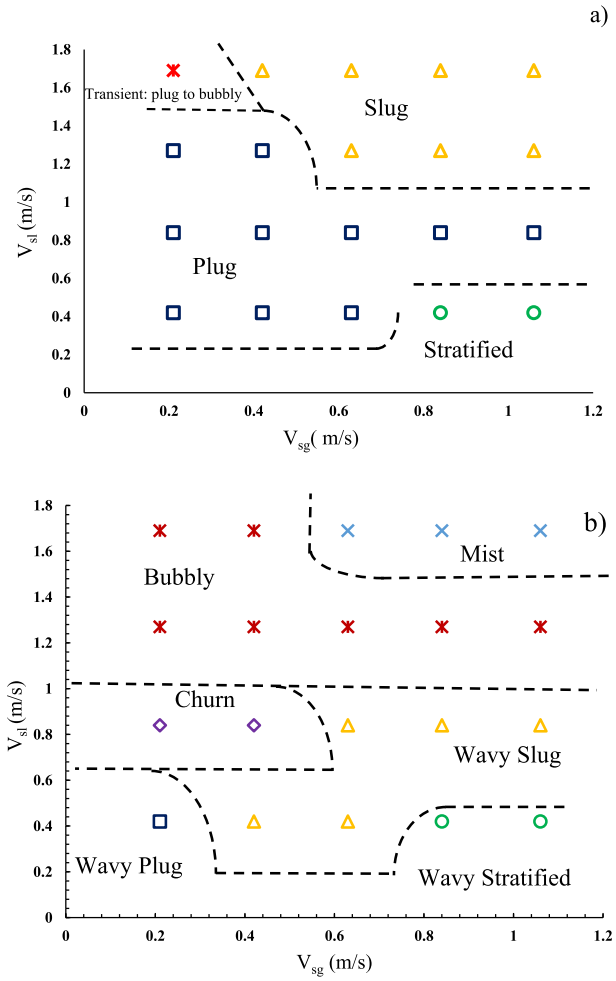

Fig. 9 Presentation of flow map for smooth tube and corrugated tube versus the superficial velocity of liquid and gas. a: Smooth tube, b: Corrugated tube.

is seen that the increment of water velocity rate causes the pressure drop ratio to decrease. The maximum and minimum pressure drop ratios were related to water superficial velocities of

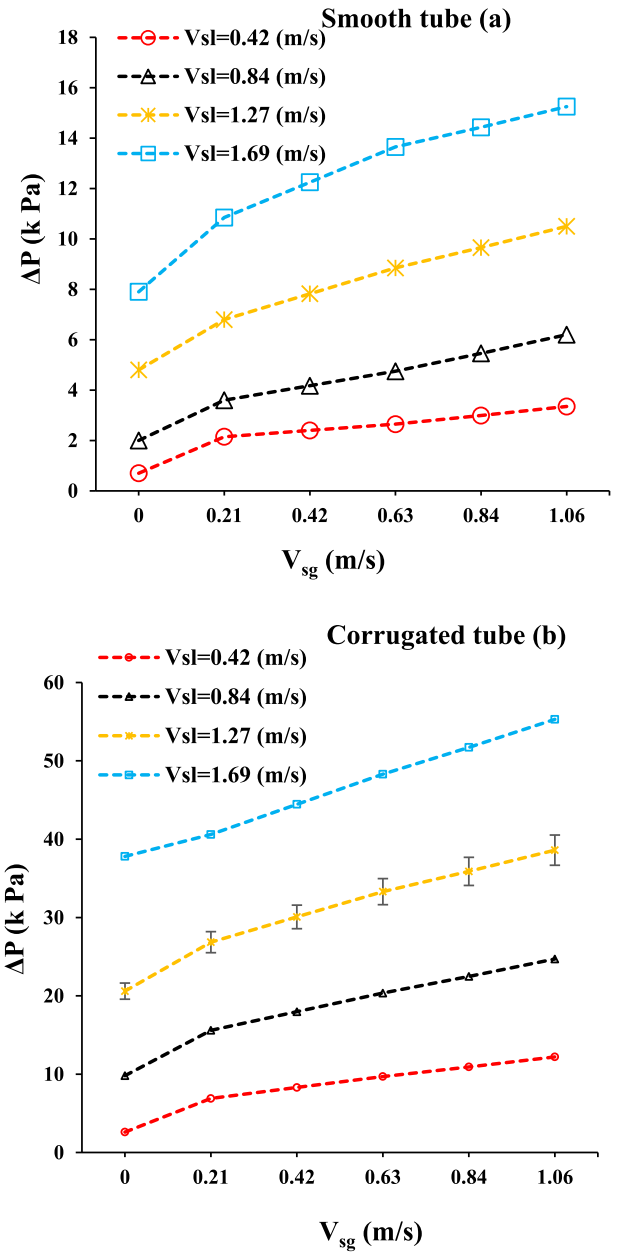

Fig. 10 Absolute amounts of pressure drop versus air superficial velocity for both smooth (a) and corrugated (b) tubes.

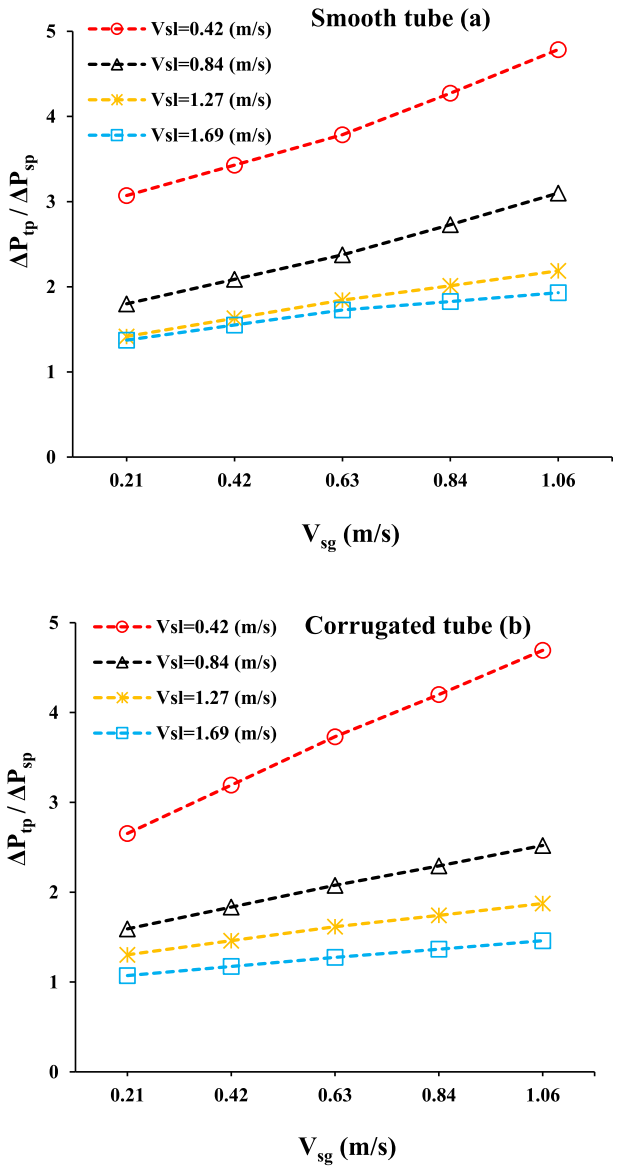

Fig. 11 Ratio of two-phase pressure drop to the single-phase pressure drop. a: Smooth tube b: corrugated tube.

0.42 and 1.69 m/s, respectively. The maximum pressure drop ratio in smooth tube was 4.8 and the minimum pressure drop ratio was 1.25, respectively. It could be explained that the following mechanisms contribute to the increment of pressure drop ratio.

- **Interaction between fluid parcels and water slugs:** As the water velocity decreases, the shear stress of the liquid phase decreases too. Subsequently, the size of slugs becomes greater and as a result, more severe interaction between the air slugs and fluid parcels occurs. This phenomenon causes more fluctuation in the liquid phase stream which results in the increment of turbulent viscosity. Subsequently, greater amount of pressure drop is observed. On

Table 3 The minimum, maximum and deviation from mean values

Water superficial velocity (m/s)	0.42			0.84			1.27			1.69		
Air superficial velocity (m/s)	0.21	0.63	1.06	0.21	0.63	1.06	0.21	0.63	1.06	0.21	0.63	1.06
Maximum pressure drop value (mbar)	72	100	132	160	212	262	271	337	390	409	488	556
Minimum pressure drop value (mbar)	66	94	112	152	195	232	266	329	382	403	478	550
Deviation from mean value (mbar)	3	3	10	4	8.5	10	2.5	4	4	3	5	3

the other hand, for the higher water velocities, the air slugs have get smaller longitudinal size and consequently minor interactions between fluid parcels and air slugs happen which lead to less pressure drop increment.

- **Increment of the local Reynolds number**: Based on the continuity principle and considering the existence of the gaseous phase, the liquid phase tends to move faster. Since the cross section for the liquid phase decreases which forces the liquid stream to move faster. This point could be explained through considering the stream of single-phase flow and a constant velocity of the liquid phase. According to the equation $Q_l = V_{l.1}A_{l.1}$, the whole cross section of the tube is for the liquid phase $(A_{l.1} = \text{crosssectionofthetube})$. By adding the second phase, the above equation for liquid phase would be written as following $Q_l = V_{l.2}A_{l.2}$. Comparing the first case and second case and assuming that the volumetric flow rate of the liquid phase is constant in both cases, it could be concluded that $V_{l.2} > V_{l.1}$. The reason behind this is that at second case, due to the existence of gaseous phase flow inside the tube, the cross-section area for the liquid phase is smaller than the first case, $(A_{l.2} < A_{l.1} = \text{wholecrosssectionofthetube})$. As a result, the local Reynolds number for each of cases increases which leads in the creation of more intensified vortices and consequently greater pressure drop. It is worth mentioning that at the operational condition of the present study both phases were considered to be incompressible.

In Fig. 11 presents the variation of pressure drop ratio (ratio of two-phase flow pressure drop to liquid single-phase flow pressure drop) versus air-velocity for both smooth and corrugated tubes. It is demonstrated that the pressure drop ratio shows similar behavior in both tubes. However, it is concluded that despite the absolute pressure drop, the pressure drop ratio in smooth tube is greater than that related to corrugated tube. The reason for this is based on the greater shear stress of the flow in the corrugated tube which disrupts the air slugs into smaller bubbles. It could be argued that the smaller bubbles in corrugated tube have less interaction with fluid parcels and less increment in pressure drop occurs in comparison with smooth tube.

3.3. Thermal analysis

In this section, the data for thermal results is discussed. The data are depicted as the variation of Nusselt number based on the corresponding superficial velocity of air and water streams. Fig. 12a presents the variation of the Nusselt number of both single phase and two-phase flow for smooth tube. It should be noted that the uncertainty values associated with the Nusselt number was $\pm 9 \cdot 75$. Also Fig. 12b presents the variation of Nu number for corrugated tube. As presented, the injection of air enhances the Nu number in comparison with single phase flow. This phenomenon is observed at both two-phase and smooth tube regardless of the ratio of enhancement. It could be explained that there is two main mechanisms that contribute in heat transfer enhancement in two-phase flow were proposed by experts [4,5,21].These mechanisms are defined as follows:

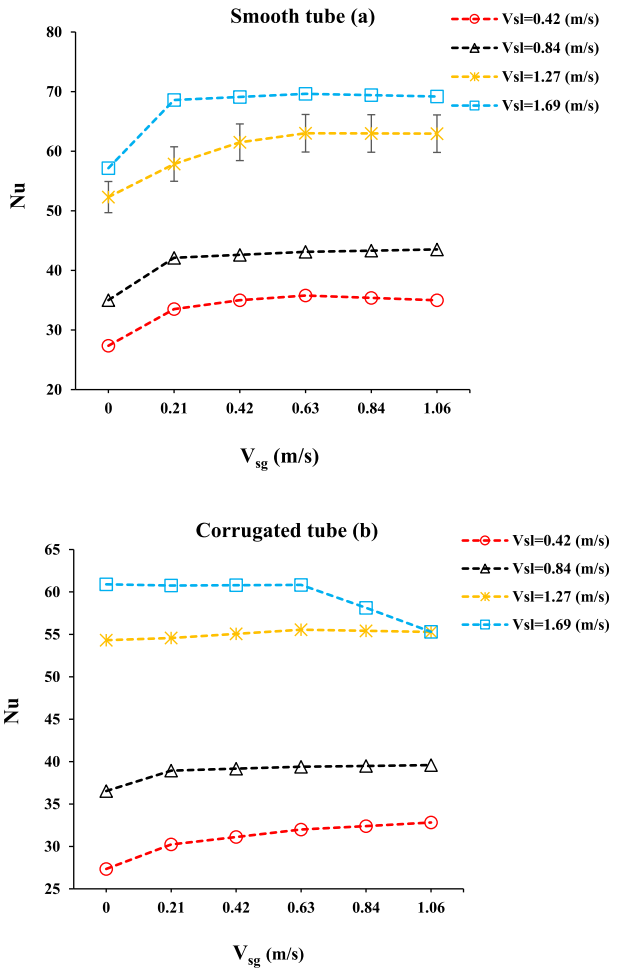

Fig. 12 Dimensionless convective heat transfer coefficient (Nu). a: Smooth tube, b: Corrugated tube.

- Increment of turbulence intensity of fluid flow due to the interaction between air bubbles/slugs and fluid parcels: These interactions increase the fluctuant terms of the velocity equation and as a result, the turbulence intensity of the flow increases. This phenomenon enhances the mixing in the boundary layer and prevents it from getting developed. Consequently, the thickness of viscous sublayer diminishes and the conductive thermal resistance of the boundary layer reduces and as a result, higher Nusselt number is obtained.
- Increment of turbulence intensity due to augmentation of local Reynolds number of the liquid phase: The addition of gaseous phase decreases the cross section of the liquid stream. Consequently, it's local velocity and local Reynolds number increases. This phenomenon also increases the mixing of fluid parcels in the boundary layer and restricts development of boundary layer.

Regarding the mechanisms mentioned above, it is expected to obtain better Nusselt number with air injection, however, it is observed in Fig. 12a that further increment of air velocity has no significant effect on the Nusselt number at the studied

range of two phase flow whereas in some points reduction in heat transfer was also observed. Although, many recent articles have mentioned the air/water two-phase flow as a useful heat transfer enhancement method, it's effectiveness is dependent on various parameters as like to flow pattern, tube orientation, frequency of the air bubbles, form and shape of the tube, etc., [6,7,19]. Comparing Fig. 12a with Fig. 9a, it could be revealed that the plug flow and slug flow are the most prevalent flow patterns observed in smooth tube in the range of liquid and air velocity considered in this study. As mentioned before, increasing the air velocity elongates the air bubbles. Although longer bubbles have positive impact on heat transfer enhancement according to the reasons mentioned above. On the other hand, they also contribute to reduction of heat transfer rate. The air bubbles lean toward the upper wall of the tube due to buoyancy effect and prevent heat transfer from the tube surface to liquid phase which is why air velocity increment remains no considerable impact on enhancement of Nu number. Also, it should be mentioned that at Vsl = 0.42 m/s further increment of air velocity results in a slight reduction of Nu number. To justify this finding, the corresponding flow pattern should be considered. As highlighted in Fig. 12a, by increasing air velocity at Vsl = 0.42 m/s stratified flow pattern was formed. Through the stratified flow about half of the tube surface is in contact with air rather than liquid. Air is known for its poor heat transfer characteristics and it is expected to observe reduction of Nusselt number in that flow regime. It is worth mentioning that the thermal behavior of two-phase flow in smooth tube at the present study was in agreement with the results of Ghajar's work [6,7].

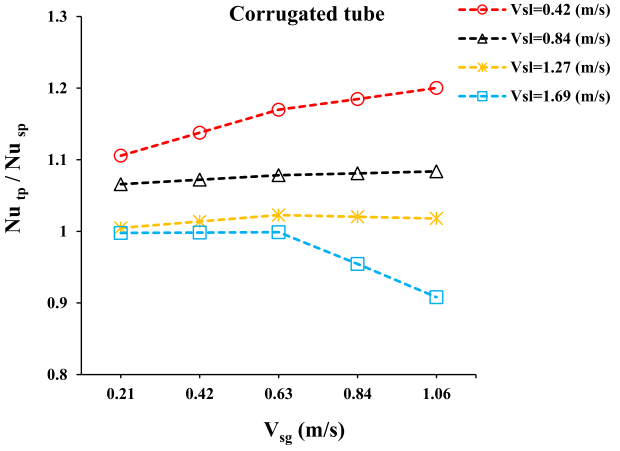

Fig. 13 Ratio of two-phase Nusselt number to single-phase Nusselt number in corrugated tube.

Fig. 12b presents the variation of Nusselt number of both single and two-phase flow in corrugated tube. Also, the Fig. 13 presents the ratio of two phase Nusselt number to that of single phase in corrugated tube. Fig. 12b indicates that for water velocity rates of Vsl = 0.42 and 0.84 m/s, the Nusselt number raises by the increment of air superficial velocity. However, further increment of air velocity doesn't effectively affect the Nusselt number. According to flow map in Fig. 9b the wavy plug/slug flow was the dominant flow patterns at water velocity rates of Vsl = 0.42,0.84 m/s whose influence on heat transfer was discussed before. It is to noted that according to the flow map of Fig. 9b at Vsl = 0.42 m/s and Vsg = 1.06 stratified wavy flow was formed. Although the Nusselt number was observed to reduce in stratified flow in smooth tube, through the corrugated tube the wavy displacement of fluid stream in the corrugated tube enhances the local contact of the liquid film with the upper surface of the tube and partially compensates for the weakness of thermal energy transfer due to vicinity of air stream with the upper wall of the tube.

In Fig. 12b. demonstrates that by raising the air velocity no significant change in Nusselt number occurs except for air velocity rates greater than 0.63 m/s and liquid velocity of 1.69 m/s. Indeed, for these velocity rates, a reduction in heat transfer was observed. To justify this finding, the flow patterns of two-phase flow should be evaluated. Fig. 9b indicates the formation of mist flow at higher liquid and air velocity rates. In this flow regime the continuous liquid film is broken and the bubbles disperse all across the flow cross section. Due to rapid movements of tiny bubbles the thermal boundary layer was dominated and liquid film loses its contact with the surface of tube where the energy is exerted to the fluid flow. Moreover, distribution of liquid droplets within the air bubbles eliminates the interaction between fluid parcels and suppresses the

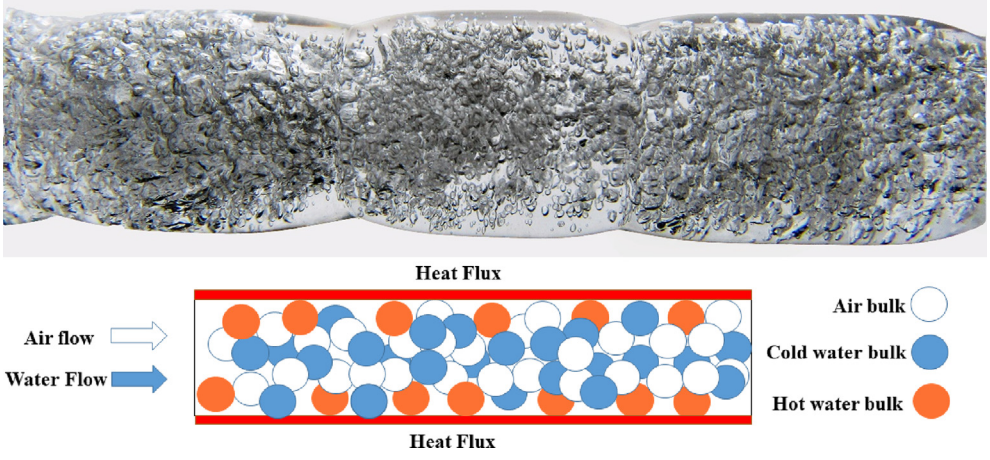

Fig. 14 Presentation of observed mist flow in corrugated tube (up) and schematic of suggested mechanism for heat transfer reduction in mist flow (down).

advective heat transfer. For the non-boiling gas–liquid two phase flow, not only the gas tiny bubble does not carry any thermal energy (opposite of what happens in flows that include phase change) but also by changing the continuum nature of the liquid phase and making it as discretized water drops, reduces the heat transfer rate between the heated walls and liquid phase. Indeed, through the mist flow, the distribution of the tiny gas bubbles increases near the heated wall. Since the thermal conductive coefficient of gas phase is so less than liquid phase the heat transfer rate reduces. Combination of these factors result in reduction of Nusselt number though the mist flow. Previous study of Gao et al [42] also reported similar findings about the reduction of heat transfer rate in mist flow. Fig. 14a depicts a closer view of the mist flow at Vsl = 1.69 m/s and Vsg = 1.06 m/s within the corrugated tube and Fig. 14b schematically illustrates the mentioned mechanism for the reduction of Nusselt number in mist flow. It should be noted that the definition of mist flow regime was based on conceptualisms made by Gao et al [42] which was based on both flow patterns (captured in numerous pictures) and thermal behavior.

4. Conclusion

The purpose of this work was to study the behavior of gas/liquid two-phase flow inside the horizontal corrugated tube. With this aim, a systematic experimental setup was fabricated and the heat transfer, flow visualization, and pressure drop experiments were conducted. The heat transfer experiments were carried out under constant heat flux. The constant heat flux was applied to the copper made smooth and corrugated tubes. Four different water superficial velocities of 0.42, 0.84, 1.27 and 1.69 m/s along with six air superficial velocities ranging from 0.21, to 1.06 m/s for each water flow rate were tested. The key findings of the present study are as follows:

- In smooth tube, four distinct flow patterns of stratified, slug, plug, and bubbly were observed. Whereas in corrugated tube stratified wavy, wavy slug, wavy plug, bubbly, churn, and mist flow regimes were observed.
- The corrugations caused wavy structure in the well-known plug and slug flow patterns. Also, the transition between flow patterns occurred more rapid than that in the smooth tube.
- The pressure drop ratio in the smooth tube was found to be greater than corrugated tube. The minimum and maximum pressure drop ratio for corrugated tube were found to be 1.07 and 4.69, respectively. Whereas, for the smooth tube these values were 1.37 and 4.78, respectively.
- In the smooth tube, at all of the liquid-phase superficial velocities, the injection of air caused the Nusselt number to enhance. The maximum increment of the Nusselt number due to the two-phase flow for the smooth tube was about 8% and was related to V_{sl} = 1.69 m/s and V_{sg} = 1.06 m/s.
- For the smooth tube, the stratified flow resulted in Nusselt number reduction. However, for corrugated tube different behavior was observed in the wavy stratified flow. It was concluded that due to wavy displacement of liquid stream in corrugated tube, the local contact of the liquid film with the upper surface of the tube was enhanced which partially compensates for the reduced transferred thermal energy.
- It was observed that there is a reduction in Nusselt number for gas superficial velocities greater than Vsg = 0.84 m/s at Vsl = 1.69 m/s. It was revealed that the mist flow was formed in the mentioned operational condition. In this flow regime the liquid phase loses its continuity and the air bubbles dominate the boundary layer. Consequently, due to higher thermal resistance of gas-phase, the heat transfer rate decreases.

Declaration of Competing Interest

The authors declare that they have no known competing financial interests or personal relationships that could have appeared to influence the work reported in this paper.

Acknowledgement

“The authors extend their appreciation to the Deanship of Scientific Research at King Khalid University for funding this work through research groups under grant number RGP.1/154/42”

References

[1] M. Sun, M. Zeng, Investigation on turbulent flow and heat transfer characteristics and technical economy of corrugated tube, Appl. Therm. Eng. 129 (2018) 1–11, https://doi.org/10.1016/j.applthermaleng.2017.09.136.
[2] A.K. Hilo, A.R. Abu Talib, A. Acosta Iborra, M.T. Hameed Sultan, M.F. Abdul Hamid, Effect of corrugated wall combined with backward-facing step channel on fluid flow and heat transfer, Energy. 190 (2020) 116294, https://doi.org/10.1016/j.energy.2019.116294.
[3] H. Peng, L. Liu, X. Ling, Y. Li, Thermo-hydraulic performances of internally finned tube with a new type wave fin arrays, Appl. Therm. Eng. 98 (2016) 1174–1188, https://doi.org/10.1016/j.applthermaleng.2015.12.115.
[4] M. Mahdi Heyhat, A. Abdi, A. Jafarzad, Performance evaluation and exergy analysis of a double pipe heat exchanger under air bubble injection, Appl. Therm. Eng. 143 (2018) 582–593, https://doi.org/10.1016/j.applthermaleng.2018.07.129.
[5] S. Khorasani, A. Moosavi, A. Dadvand, M. Hashemian, A comprehensive second law analysis of coil side air injection in the shell and coiled tube heat exchanger: An experimental study, Appl. Therm. Eng. 150 (2019) 80–87, https://doi.org/10.1016/j.applthermaleng.2018.12.163.
[6] D. Kim, A.J. Ghajar, Heat transfer measurements and correlations for air–water flow of different flow patterns in a horizontal pipe, Exp. Therm. Fluid Sci. 25 (8) (2002) 659–676, https://doi.org/10.1016/S0894-1777(01)00120-0.
[7] J.-Y. Kim, A.J. Ghajar, A general heat transfer correlation for non-boiling gas–liquid flow with different flow patterns in horizontal pipes, Int. J. Multiph. Flow. 32 (4) (2006) 447–465, https://doi.org/10.1016/j.ijmultiphaseflow.2006.01.002.
[8] J. López, H. Pineda, D. Bello, N. Ratkovich, Study of liquid–gas two-phase flow in horizontal pipes using high speed filming and computational fluid dynamics, Exp. Therm. Fluid Sci. 76 (2016) 126–134, https://doi.org/10.1016/j.expthermflusci.2016.02.013.
[9] J. Thaker, J. Banerjee, On intermittent flow characteristics of gas–liquid two-phase flow, Nucl. Eng. Des. 310 (2016) 363–377, https://doi.org/10.1016/j.nucengdes.2016.10.020.
[10] R. Ibarra, J. Nossen, M. Tutkun, Two-phase gas-liquid flow in concentric and fully eccentric annuli. Part I: Flow patterns,

holdup, slip ratio and pressure gradient, Chem. Eng. Sci. 203 (2019) 489–500, https://doi.org/10.1016/j.ces.2019.01.064.
[11] R. Ibarra, J. Nossen, M. Tutkun, Two-phase gas-liquid flow in concentric and fully eccentric annuli. Part II: Model development, flow regime transition algorithm and pressure gradient, Chem. Eng. Sci. 203 (2019) 501–510, https://doi.org/10.1016/j.ces.2019.02.021.
[12] S.M. Bhagwat, A.J. Ghajar, Experimental investigation of non-boiling gas-liquid two phase flow in downward inclined pipes, Exp. Therm. Fluid Sci. 89 (2017) 219–237, https://doi.org/10.1016/j.expthermflusci.2017.08.020.
[13] S.M. Bhagwat, A.J. Ghajar, Experimental investigation of non-boiling gas-liquid two phase flow in upward inclined pipes, Exp. Therm. Fluid Sci. 79 (2016) 301–318, https://doi.org/10.1016/j.expthermflusci.2016.08.004.
[14] H. Liu, T. Hibiki, Flow regime transition criteria for upward two-phase flow in vertical rod bundles, Int. J. Heat Mass Transf. 108 (2017) 423–433, https://doi.org/10.1016/j.ijheatmasstransfer.2016.12.029.
[15] B. Wu, M. Firouzi, T.E. Rufford, B. Towler, Characteristics of counter-current gas-liquid two-phase flow and its limitations in vertical annuli, Exp. Therm. Fluid Sci. 109 (2019) 109899, https://doi.org/10.1016/j.expthermflusci.2019.109899.
[16] A.M. Aliyu, Y.D. Baba, L. Lao, H. Yeung, K.C. Kim, Interfacial friction in upward annular gas–liquid two-phase flow in pipes, Exp. Therm. Fluid Sci. 84 (2017) 90–109, https://doi.org/10.1016/j.expthermflusci.2017.02.006.
[17] R. Guo, Y. Chen, P.J. Waltrich, W.C. Williams, An experimental investigation on flow pattern map and drift-flux model for co-current upward liquid-gas two-phase flow in narrow annuli, J. Nat. Gas Sci. Eng. 51 (2018) 65–72, https://doi.org/10.1016/j.jngse.2017.12.025.
[18] X. Shen, J.P. Schlegel, T. Hibiki, H. Nakamura, Some characteristics of gas–liquid two-phase flow in vertical large-diameter channels, Nucl. Eng. Des. 333 (2018) 87–98, https://doi.org/10.1016/j.nucengdes.2018.04.001.
[19] M. Gourma, P.G. Verdin, Two-phase slug flows in helical pipes: Slug frequency alterations and helicity fluctuations, Int. J. Multiph. Flow. 86 (2016) 10–20, https://doi.org/10.1016/j.ijmultiphaseflow.2016.07.013.
[20] G. Zhu, X. Yang, S. Jiang, H. Zhu, Intermittent gas-liquid two-phase flow in helically coiled tubes, Int. J. Multiph. Flow. 116 (2019) 113–124, https://doi.org/10.1016/j.ijmultiphaseflow.2019.04.013.
[21] H. Moradi, A. Bagheri, M. Shafaee, S. Khorasani, Experimental investigation on the thermal and entropic behavior of a vertical helical tube with none-boiling upward air-water two-phase flow, Appl. Therm. Eng. 157 (2019) 113621, https://doi.org/10.1016/j.applthermaleng.2019.04.031.
[22] C. Zhang, D. Wang, S. Xiang, Y. Han, X. Peng, Numerical investigation of heat transfer and pressure drop in helically coiled tube with spherical corrugation, Int. J. Heat Mass Transf. 113 (2017) 332–341, https://doi.org/10.1016/j.ijheatmasstransfer.2017.05.108.
[23] H. Sadighi Dizaji, S. Jafarmadar, F. Mobadersani, Experimental studies on heat transfer and pressure drop characteristics for new arrangements of corrugated tubes in a double pipe heat exchanger, Int. J. Therm. Sci. 96 (2015) 211–220, https://doi.org/10.1016/j.ijthermalsci.2015.05.009.
[24] C. Qi, Y.-L. Wan, C.-Y. Li, D.-T. Han, Z.-H. Rao, Experimental and numerical research on the flow and heat transfer characteristics of TiO2-water nanofluids in a corrugated tube, Int. J. Heat Mass Transf. 115 (2017) 1072–1084, https://doi.org/10.1016/j.ijheatmasstransfer.2017.08.098.
[25] F. Andrade, A.S. Moita, A. Nikulin, A.L.N. Moreira, H. Santos, Experimental investigation on heat transfer and pressure drop of internal flow in corrugated tubes, Int. J. Heat Mass Transf. 140 (2019) 940–955, https://doi.org/10.1016/j.ijheatmasstransfer.2019.06.025.
[26] R.K. Ajeel, W.-S.-I.-W. Salim, K. Hasnan, Influences of geometrical parameters on the heat transfer characteristics through symmetry trapezoidal-corrugated channel using SiO2-water nanofluid, Int. Commun. Heat Mass Transf. 101 (2019) 1–9, https://doi.org/10.1016/j.icheatmasstransfer.2018.12.016.
[27] F. Xin, Z. Liu, N. Zheng, P. Liu, W. Liu, Numerical study on flow characteristics and heat transfer enhancement of oscillatory flow in a spirally corrugated tube, Int. J. Heat Mass Transf. 127 (2018) 402–413, https://doi.org/10.1016/j.ijheatmasstransfer.2018.06.139.
[28] Y. Cao, P.T. Nguyen, K. Jermsittiparsert, H. Belmabrouk, S. O. Alharbi, M.S. Khorasani, Thermal characteristics of air-water two-phase flow in a vertical annularly corrugated tube, J. Energy Storage. 31 (2020), https://doi.org/10.1016/j.est.2020.101605.
[29] T. Dagdevir, V. Ozceyhan, An experimental study on heat transfer enhancement and flow characteristics of a tube with plain, perforated and dimpled twisted tape inserts, Int. J. Therm. Sci. 159 (2021) 106564, https://doi.org/10.1016/j.ijthermalsci.2020.106564.
[30] T. Dagdevir, M. Uyanik, V. Ozceyhan, The experimental thermal and hydraulic performance analyses for the location of perforations and dimples on the twisted tapes in twisted tape inserted tube, Int. J. Therm. Sci. 167 (2021) 107033, https://doi.org/10.1016/j.ijthermalsci.2021.107033.
[31] S.P. Nalavade, P.W. Deshmukh, N.K. Sane, Heat transfer and friction factor characteristics of turbulent flow using thermally non conductive twisted tape inserts, Mater. Today Proc. (2021), https://doi.org/10.1016/j.matpr.2021.09.061.
[32] S. Rostami, N. Ahmadi, S. Khorasani, Experimental investigations of thermo-exergitic behavior of a four-start helically corrugated heat exchanger with air/water two-phase flow, Int. J. Therm. Sci. 145 (2019) 106030, https://doi.org/10.1016/j.ijthermalsci.2019.106030.
[33] B. Abdzadeh, A. Hosainpour, S. Jafarmadar, F. Sharifian, Thermo-entropic evaluation of the effect of air injection into horizontal helical tube, J. Energy Storage. 38 (2021) 102542, https://doi.org/10.1016/j.est.2021.102542.
[34] R.J. Moffat, Describing the uncertainties in experimental results, Exp. Therm. Fluid Sci. 1 (1) (1988) 3–17, https://doi.org/10.1016/0894-1777(88)90043-X.
[35] F.P. Incropera, D.P. DeWitt, Fundamentals of Heat and Mass Transfer (1996) 890. doi: 10.1016/j.applthermaleng.2011.03.022.
[36] A.J. Kalapatapu, S.; Bhagwat, S.M.; Oyewole, A.; Ghajar, Non-boiling heat transfer in horizontal and near horizontal upward inclined gas-liquid two phase flow, in: 10th Int. Conf. Heat Transf. Fluid Mech. Thermodyn. 2014. (2014).
[37] M. Abdulkadir, D. Zhao, L.A. Abdulkareem, N.O. Asikolaye, V. Hernandez-Perez, Insights into the transition from plug to slug flow in a horizontal pipe: An experimental study, Chem. Eng. Res. Des. 163 (2020) 85–95, https://doi.org/10.1016/j.cherd.2020.08.025.
[38] M. Darzi, C. Park, Numerical investigation of horizontal two-phase plug/bubble flows: Gravitational effect on hydrodynamic characteristics, Eur. J. Mech. - B/Fluids. 74 (2019) 342–350, https://doi.org/10.1016/j.euromechflu.2018.09.006.
[39] N. Sinaga, S. khorasani, K. Sooppy Nisar, A. Kaood, Second law efficiency analysis of air injection into inner tube of double tube heat exchanger, Alexandria Eng, J. 60 (1) (2021) 1465–1476, https://doi.org/10.1016/j.aej.2020.10.064.
[40] P. Sassi, Y. Stiriba, J. Lobera, V. Palero, J. Pallarès, Experimental Analysis of Gas–Liquid–Solid Three-Phase Flows in Horizontal Pipelines, Flow Turbul. Combust. 105 (4) (2020) 1035–1054, https://doi.org/10.1007/s10494-020-00141-1.

[41] G. Montoya, D. Lucas, E. Baglietto, Y. Liao, A review on mechanisms and models for the churn-turbulent flow regime, Chem. Eng. Sci. 141 (2016) 86–103, https://doi.org/10.1016/j.ces.2015.09.011.

[42] Y. Gao, Y. Cui, B. Xu, B. Sun, X. Zhao, H. Li, L. Chen, Two phase flow heat transfer analysis at different flow patterns in the wellbore, Appl. Therm. Eng. 117 (2017) 544–552, https://doi.org/10.1016/j.applthermaleng.2017.02.058.